



A perspective on Organic Photovoltaics

Garry Rumbles

21st

- Research cell efficiencies
- Driving force for electron transfer and the relationship to V_{oc}
- Charge-Transfer states, Charge-Separated states, and the state of separated charges
- IP , E_A , ν E_{ox} , E_{red}

Funding by the Solar Photochemistry Program
Division of Chemical Sciences, Geosciences, and Biosciences

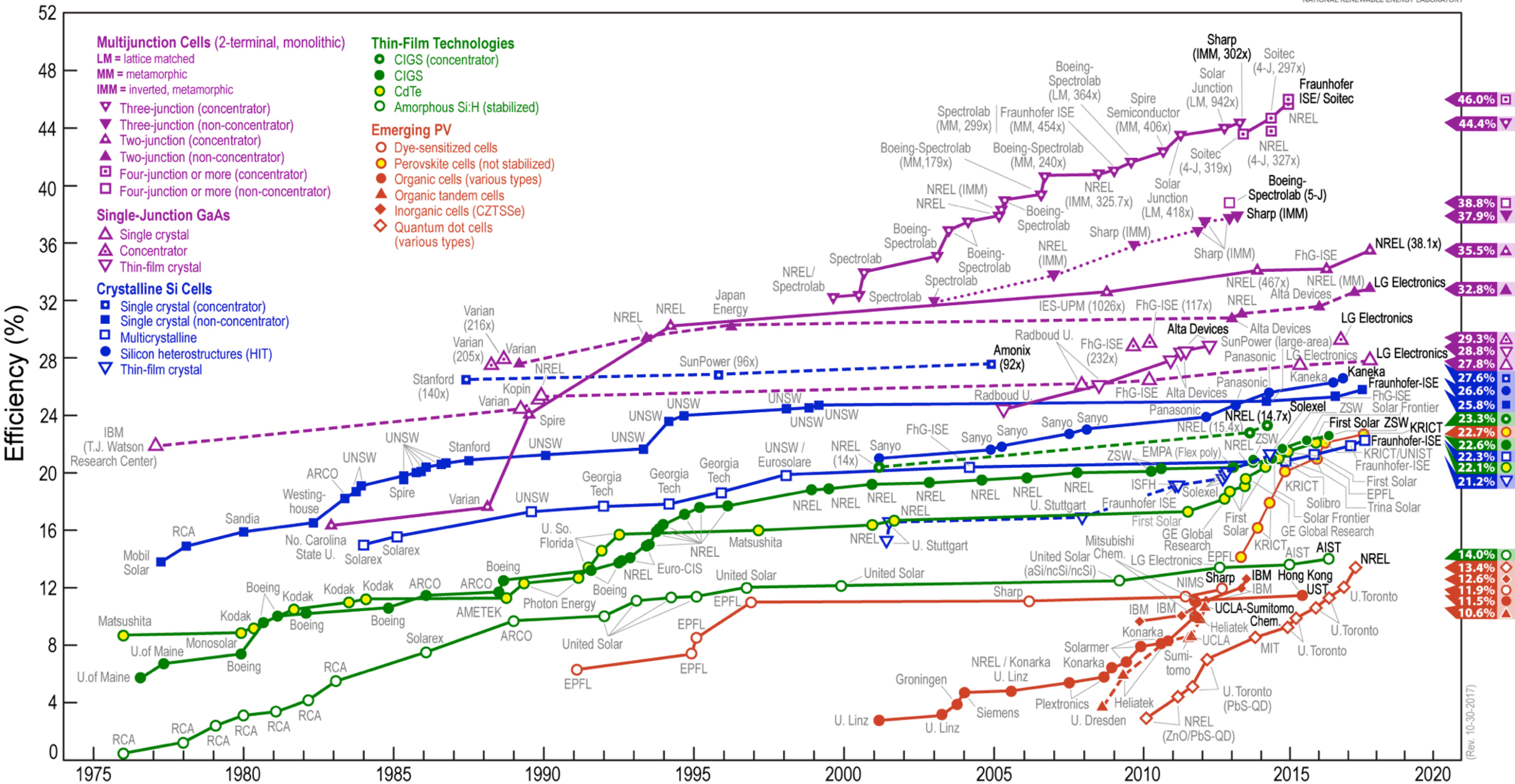


U.S. DEPARTMENT OF
ENERGY

Office of
Science

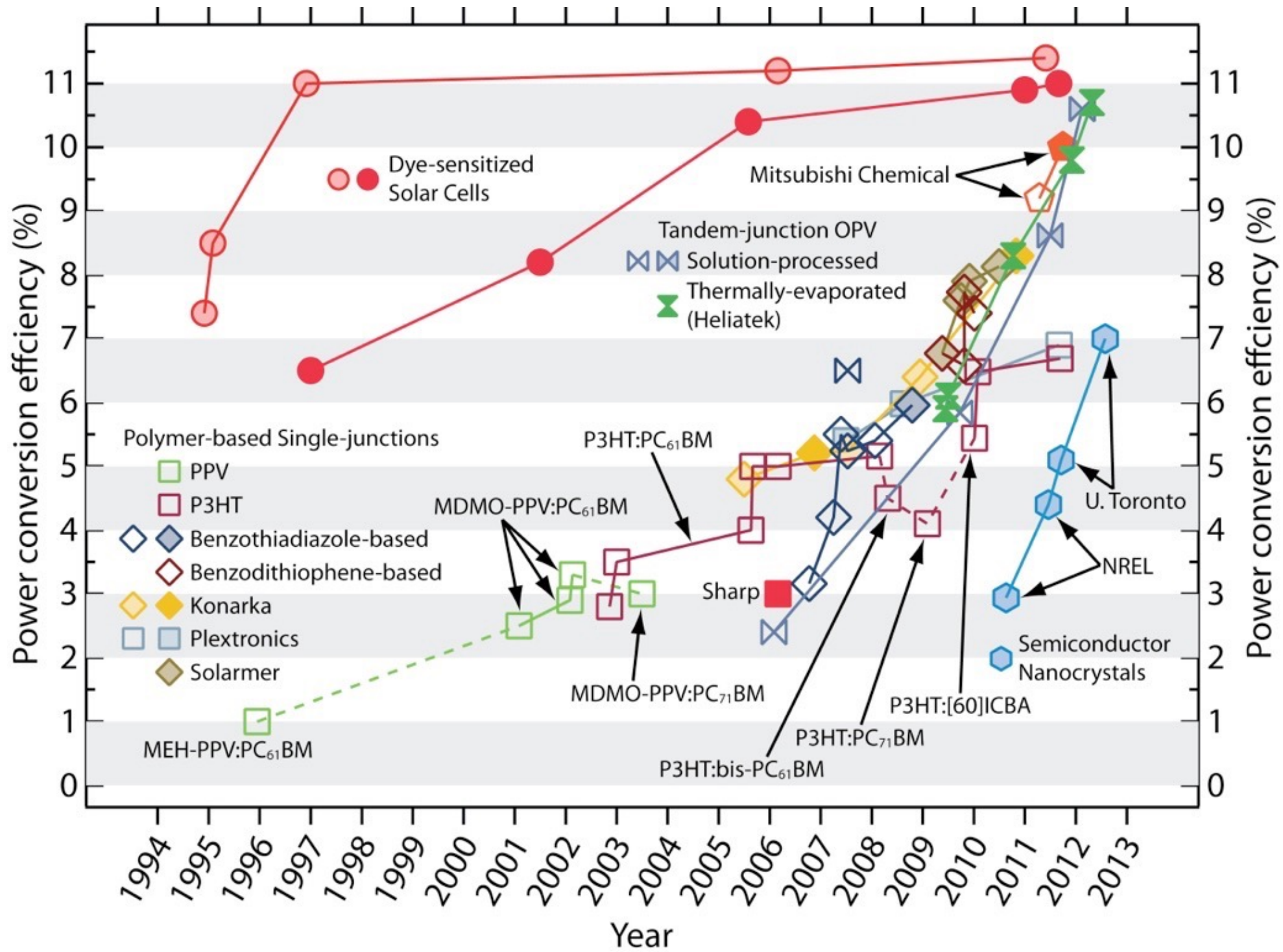


Best Research-Cell Efficiencies



NREL efficiency chart (<https://www.nrel.gov/pv/assets/images/efficiency-chart.png>)

(Rev. 10-30-2017)



Interactive: Record-Breaking PV Cells

The world's leading PV research labs use this chart to track record-breaking solar cells. New champs appear as soon as they are certified

There's often a lot of hype when solar companies claim to set new records. But to see how different PV technologies really stack up, it's important to compare standardized and independent efficiency tests. Here, we present the records that have been independently verified by [the world's three leading independent labs](#).

For explanation of the cell types, cell categories, and additional analysis, please see ["What Makes a Good PV Technology?"](#)

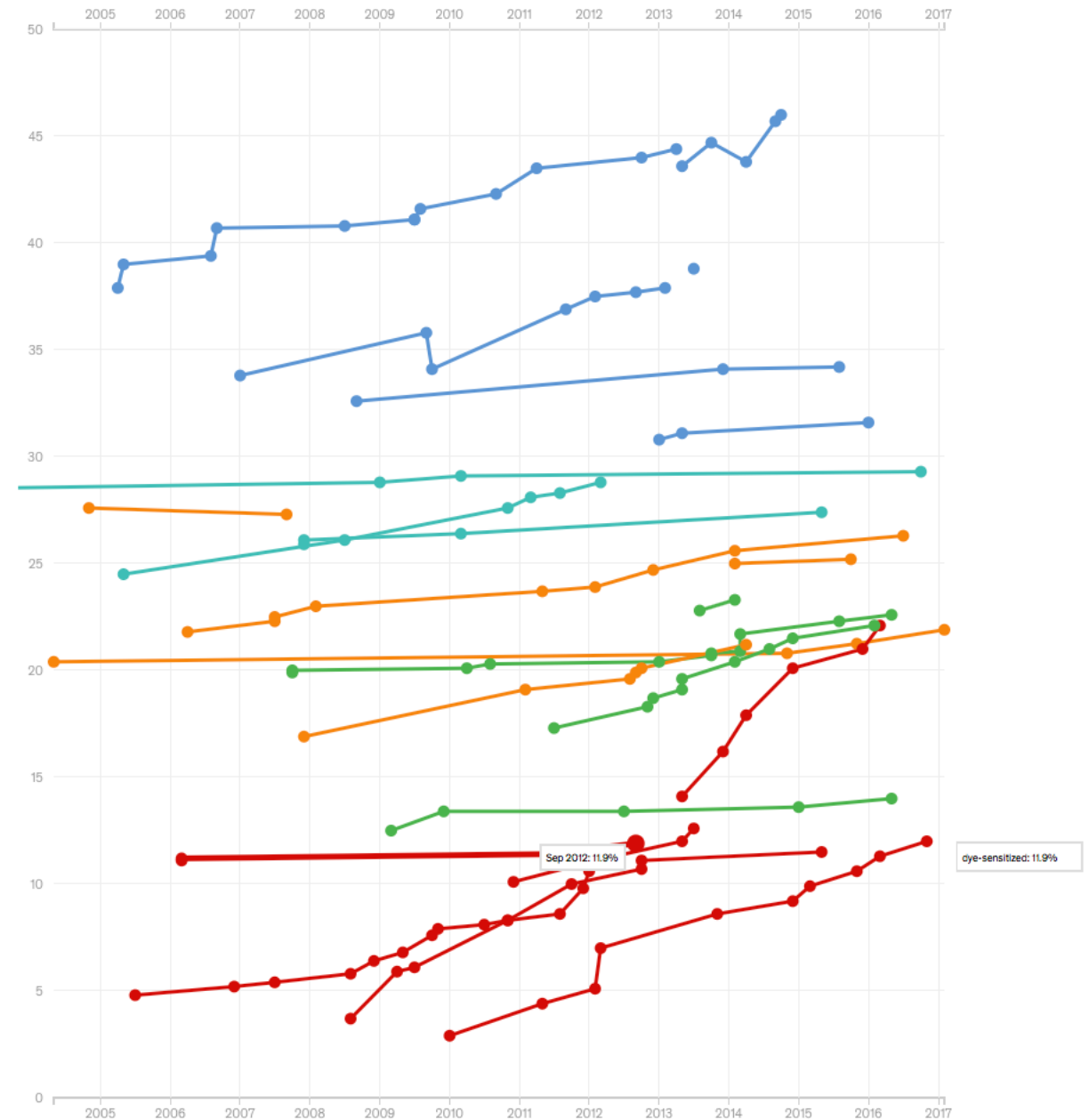
Due to the dense nature of the data, this graphic is best viewed on a large display.

Best Research Cell Efficiencies (Version: 2017-09-21)

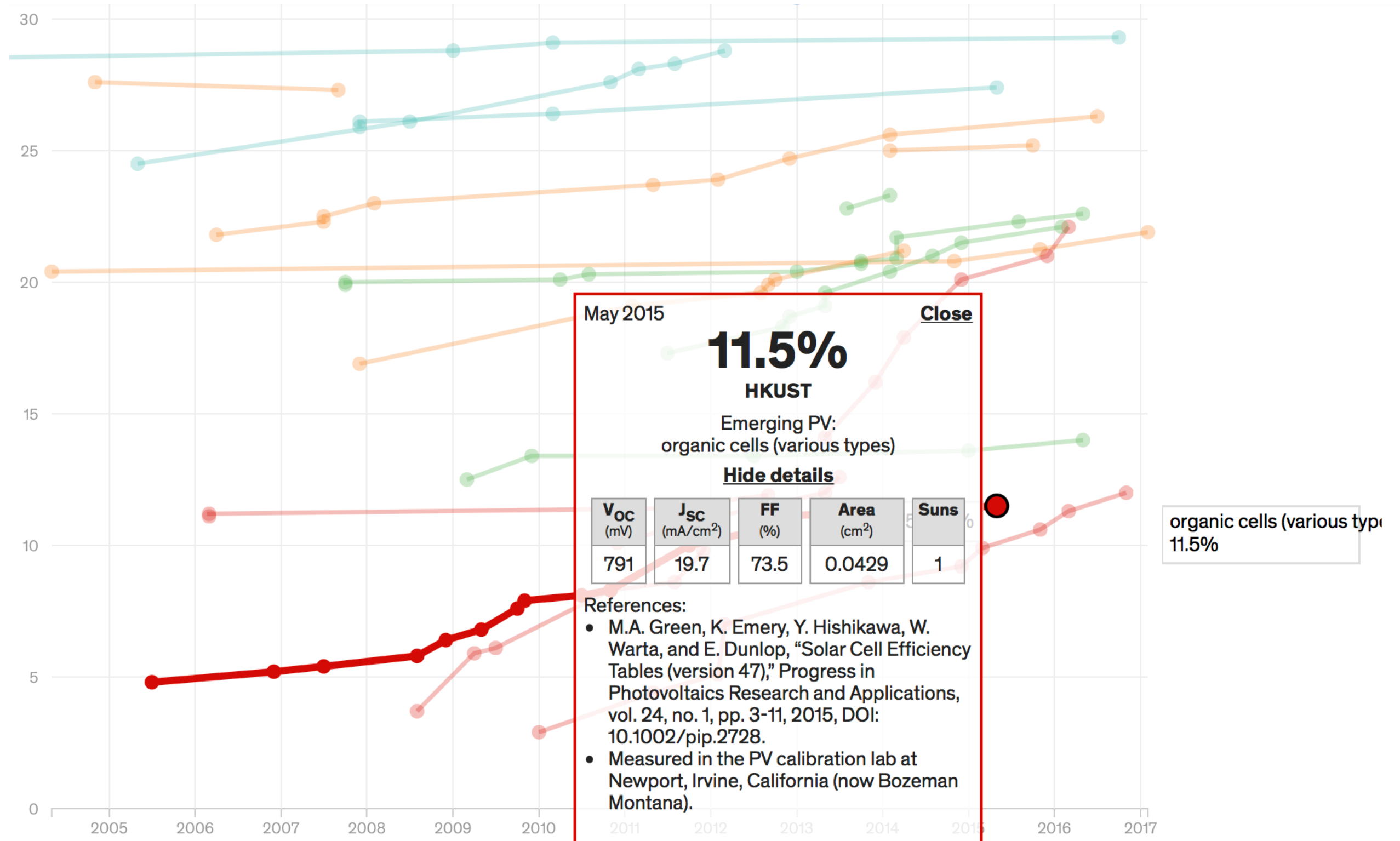
Each line on the chart represents a different type of PV cell, and each dot represents a new verified efficiency record. Lines are colored according to the five categories of cells listed below.

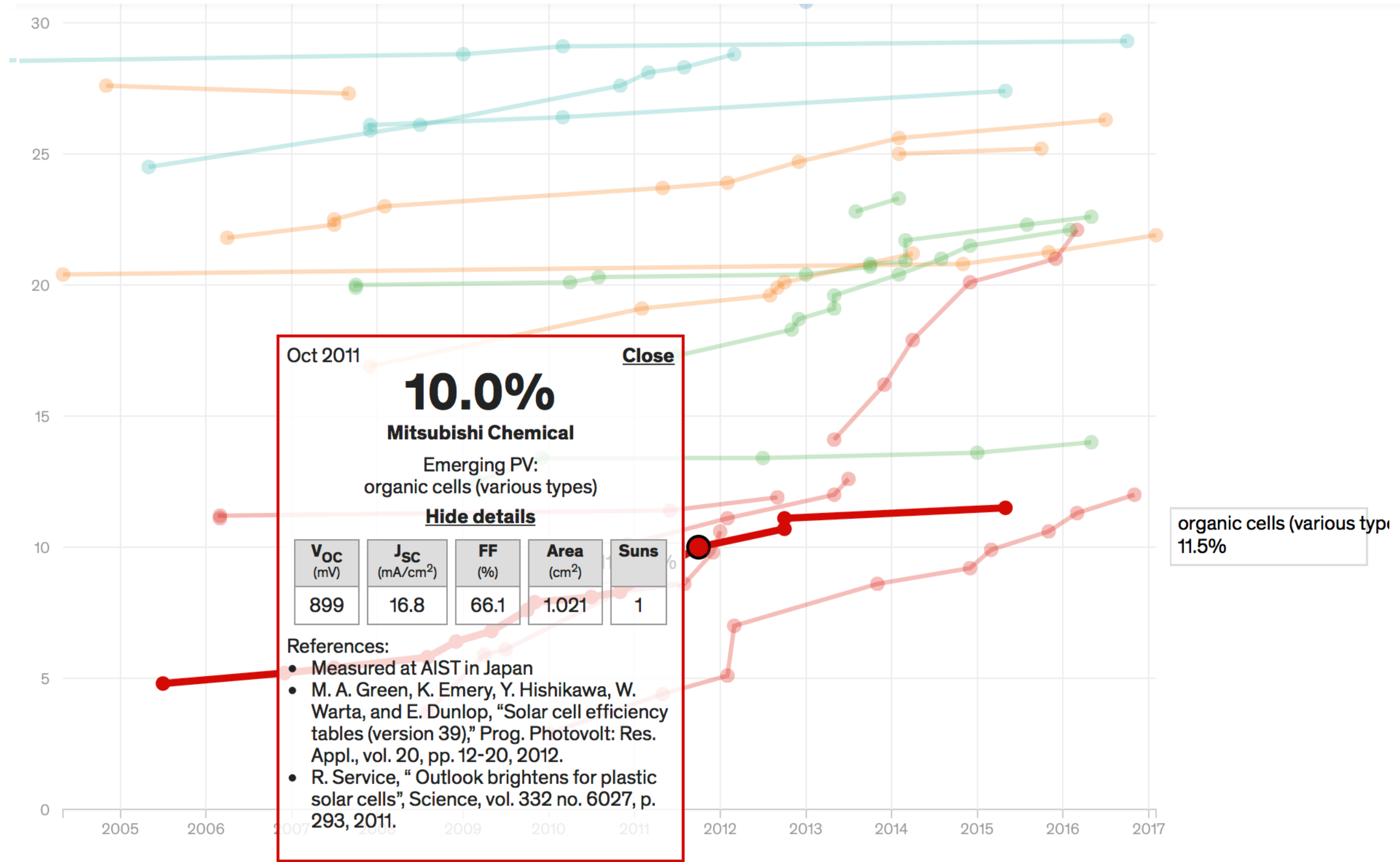
● Crystalline Si Cells ● Emerging PV ● Multijunction Cells ● Single-junction GaAs ● Thin-film Technologies

Click any dot to see the detailed information about that record.



Credit: IEEE Spectrum/NREL. Infographic: Josh Romero





Received: 4 November 2017 | Accepted: 17 November 2017

DOI: 10.1002/pip.2978

WILEY **PROGRESS IN PHOTOVOLTAICS****ACCELERATED PUBLICATION****Solar cell efficiency tables (version 51)**

Martin A. Green¹  | Yoshihiro Hishikawa²  | Ewan D. Dunlop³ | Dean H. Levi⁴ |
 Jochen Hohl-Ebinger⁵ | Anita W.Y. Ho-Baillie¹ 

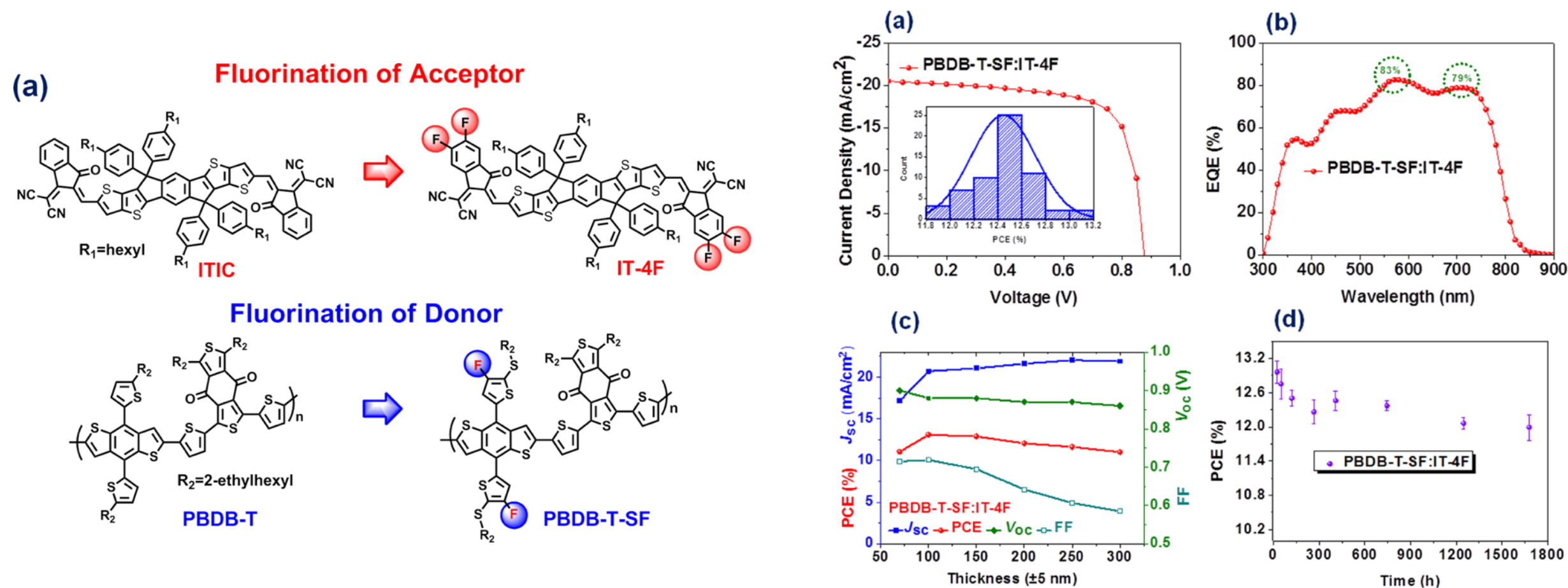
¹ Australian Centre for Advanced Photovoltaics, University of New South Wales, Sydney, 2052, Australia² Research Center for Photovoltaics (RCPV), National Institute of Advanced Industrial Science and Technology (AIST), Central 2, Umezono 1-1-1, Tsukuba, Ibaraki, 305-8568, Japan³ Directorate C—Energy, Transport and Climate, European Commission—Joint Research Centre, Via E. Fermi 2749, IT-21027 Ispra, VA, Italy⁴ National Renewable Energy Laboratory, 15013 Denver West Parkway, Golden, CO 80401, USA⁵ Department of Characterisation and Simulation/CalLab Cells, Fraunhofer-Institute for Solar Energy Systems, Heidenhofstraße 2, D-79110 Freiburg, Germany

TABLE 4 “Notable exceptions”: “Top 10” confirmed cell and module results not class records measured under the global AM1.5 spectrum (1000 Wm⁻²) at 25°C (IEC 60904-3: 2008, ASTM G-173-03 global)

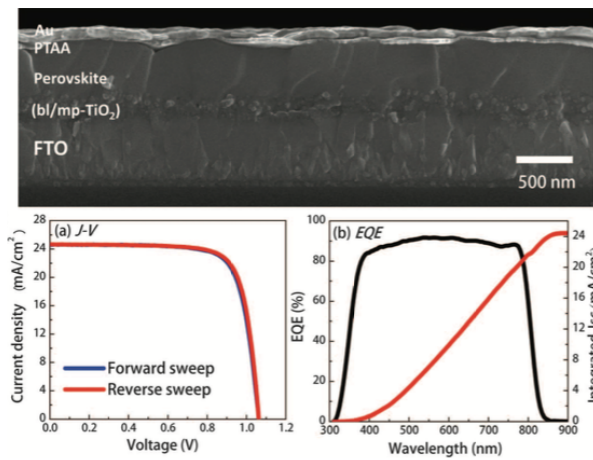
Classification	Efficiency, %	Area, cm ²	V _{oc} , V	J _{sc} , mA/cm ²	Fill Factor, %	Test Centre (date)	Description
Cells (silicon)							
Si (crystalline)	25.0 ± 0.5	4.00 (da)	0.706	42.7 ^a	82.8	Sandia (3/99) ^b	UNSW p-type PERC top/rear contacts ³⁷
Si (crystalline)	25.8 ± 0.5 ^c	4.008 (da)	0.7241	42.87 ^d	83.1	FhG-ISE (7/17)	FhG-ISE, n-type top/rear contacts ³⁸
Si (large)	26.6 ± 0.5	179.74 (da)	0.7403	42.5 ^e	84.7	FhG-ISE (11/16)	Kaneka, n-type rear IBC ³
Si (multicrystalline)	22.0 ± 0.4	245.83 (t)	0.6717	40.55 ^d	80.9	FhG-ISE (9/17)	Jinko solar, large p-type ³⁹
GaInP	21.4 ± 0.3	0.2504 (ap)	1.4932	16.31 ^f	87.7	NREL (9/16)	LG electronics, high bandgap ⁴⁰
GaInAsP/GaInAs	32.6 ± 1.4 ^c	0.248 (ap)	2.024	19.51 ^d	82.5	NREL (10/17)	NREL, monolithic tandem
Cells (chalcogenide)							
CIGS (thin-film)	22.6 ± 0.5	0.4092 (da)	0.7411	37.76 ^f	80.6	FhG-ISE (2/16)	ZSW on glass ⁴¹
CIGSS (cd free)	22.0 ± 0.5	0.512 (da)	0.7170	39.45 ^f	77.9	FhG-ISE (2/16)	Solar frontier on glass ¹⁰
CdTe (thin-film)	22.1 ± 0.5	0.4798 (da)	0.8872	31.69 ^g	78.5	Newport (11/15)	First solar on glass ⁴²
CZTSS (thin-film)	12.6 ± 0.3	0.4209 (ap)	0.5134	35.21 ^h	69.8	Newport (7/13)	IBM solution grown ⁴³
CZTS (thin-film)	11.0 ± 0.2	0.2339 (da)	0.7306	21.74 ^e	69.3	NREL (3/17)	UNSW on glass ¹²
Cells (other)							
Perovskite (thin-film)	22.7 ± 0.8 ⁱ	0.0935 (ap)	1.144	24.92 ^d	79.6	Newport (7/17)	KRICT ¹⁵
Organic (thin-film)	12.1 ± 0.3 ^k	0.0407 (ap)	0.8150	20.27 ^e	73.5	Newport (2/17)	Phillips 66

Non-fullerene acceptors

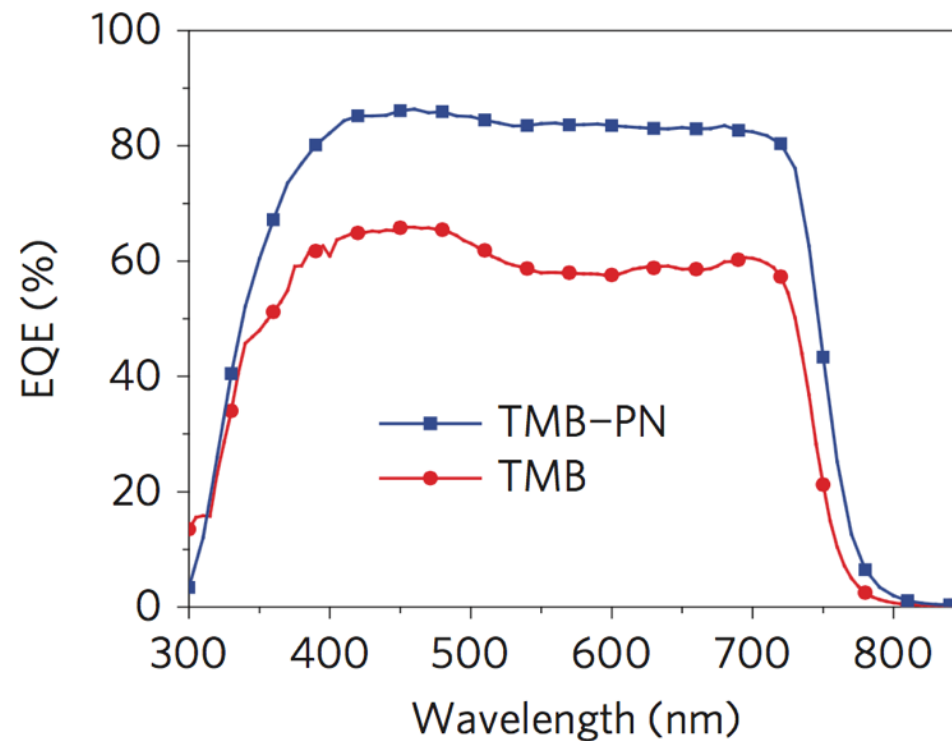
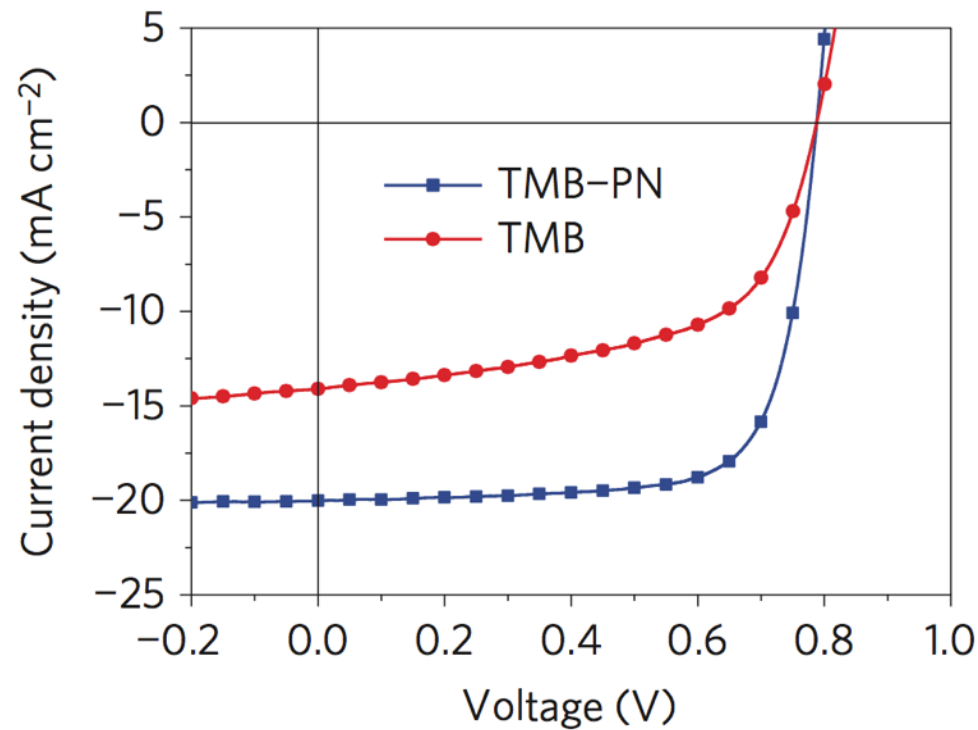
Zhao, W.; Li, S.; Yao, H.; Zhang, S.; Zhang, Y.; Yang, B.; Hou, J.
Molecular Optimization Enables Over 13% Efficiency in Organic Solar Cells.
J Am Chem Soc 2017, 139 (21), 7148–7151.



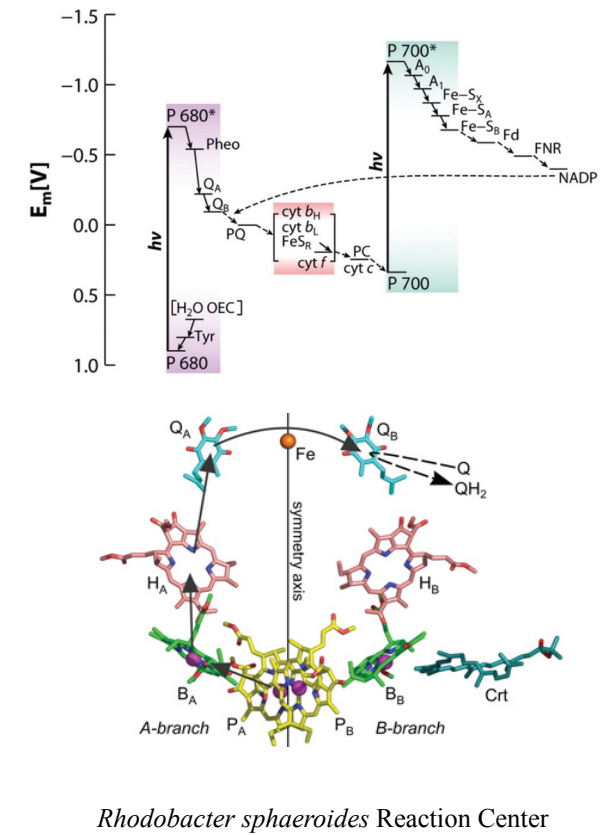
‘Consequently, an impressive PCE of 13.0% was recorded for the PBDB-T-SF:IT-4F-based device, which was certified as 13.1% by the **National Institute of Metrology, China (NIM)**, suggesting that the results obtained in our lab are reliable.’



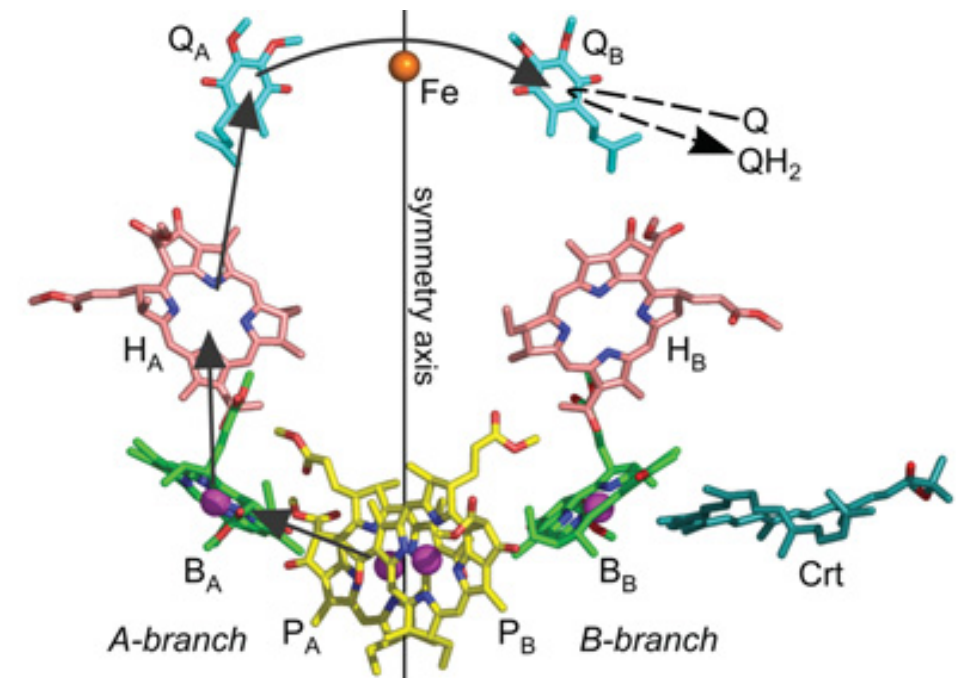
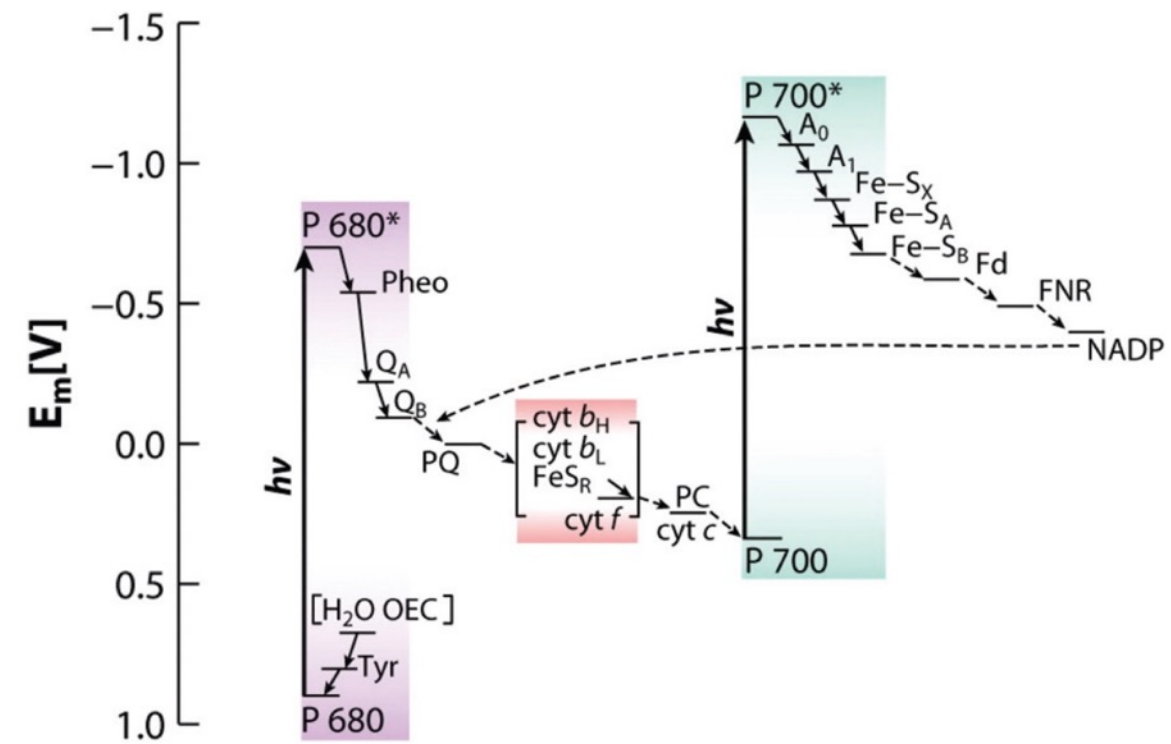
Yang, W. S.; Noh, J. H.; Jeon, N. J.; Kim, Y. C.; Ryu, S.; Seo, J.; Seok, S. I.
High-Performance Photovoltaic Perovskite Layers Fabricated Through Intramolecular Exchange.
Science **2015**, 348, 1234–1237.



Zhao, J.; Li, Y.; Yang, G.; Jiang, K.; Lin, H.; Ade, H.; Ma, W.; Yan, H.
Efficient Organic Solar Cells Processed From Hydrocarbon Solvents.
Nat. Energy **2016**, 1, 15027.

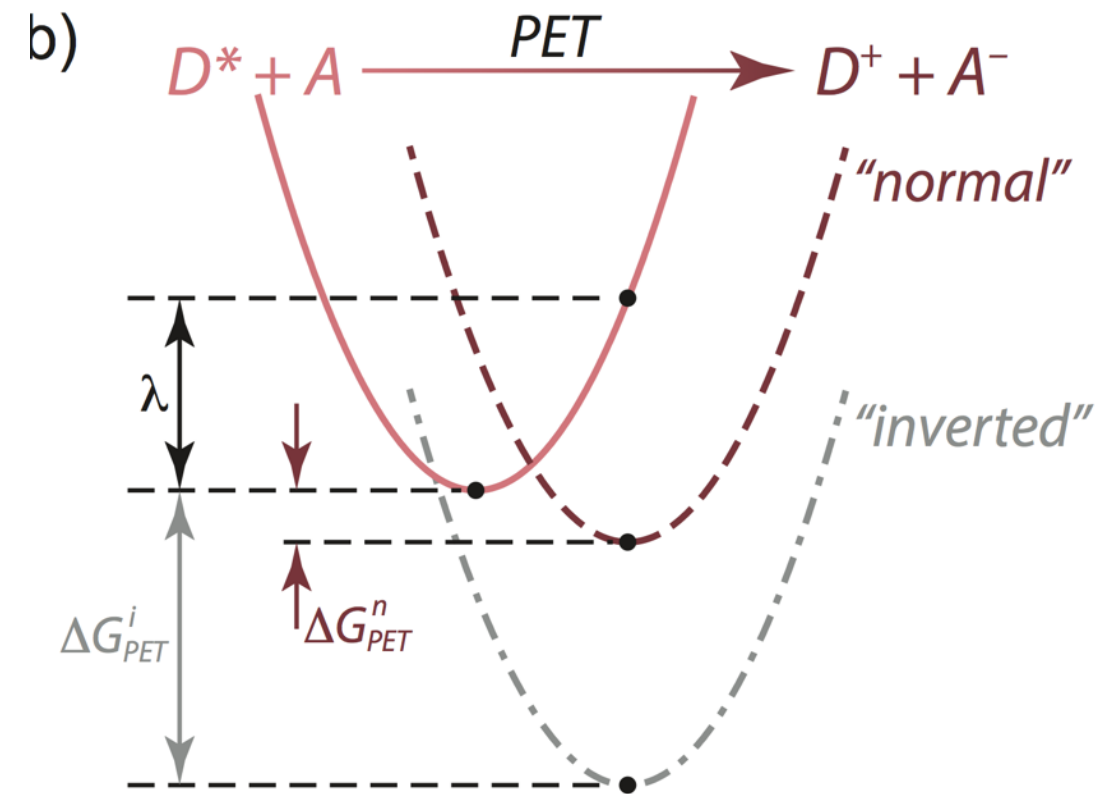


- Connect molecular, photo-induced electron transfer theory to the bulk heterojunction solar cell
- Identify role of states intermediate between excitation and free carriers
- Establish the nature of the pathway(s) for recombination
- Understand the role of solid-state microstructure



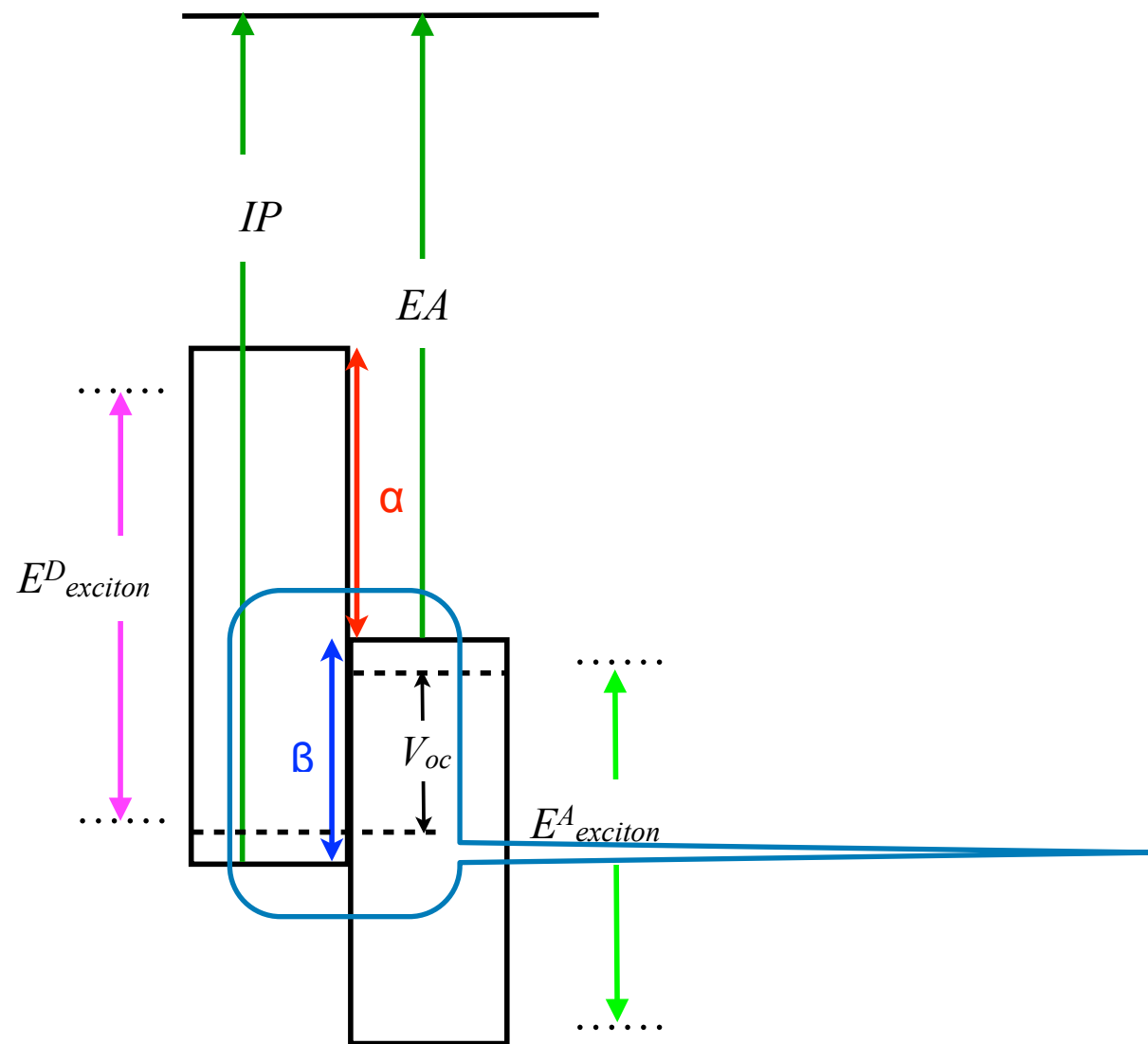
Rhodobacter sphaeroides Reaction Center

- Connect molecular, photo-induced electron transfer theory to the bulk heterojunction solar cell
- Identify role of states intermediate between excitation and free carriers
- Establish the nature of the pathway(s) for recombination
- Understand the role of solid-state microstructure



$$k_{ET} = \frac{2\pi}{\hbar} |H_{AB}|^2 \frac{1}{\sqrt{4\pi\lambda k_B T}} \exp\left(-\frac{(\lambda + \Delta G^o)^2}{4\lambda k_B T}\right)$$

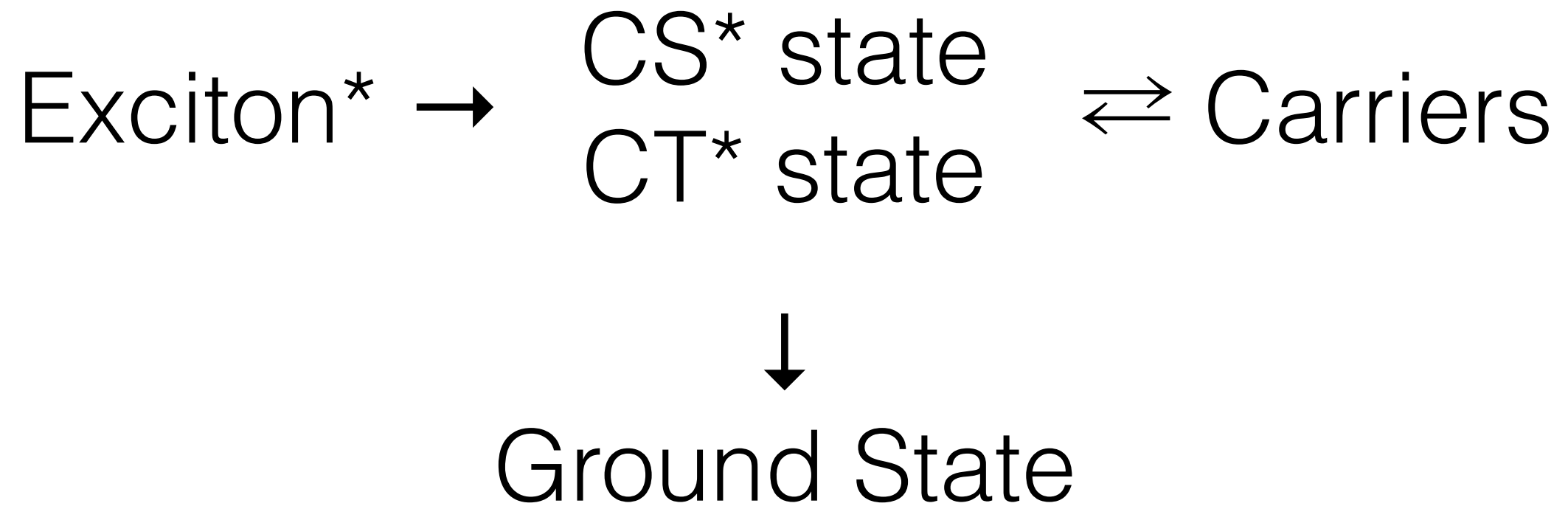
Why is this important? (Using type II model)



$$\alpha = LUMO_{Acceptor} - LUMO_{Donor}$$

$$\beta = LUMO_{Acceptor} - HOMO_{Donor}$$
$$\approx V_{oc}$$

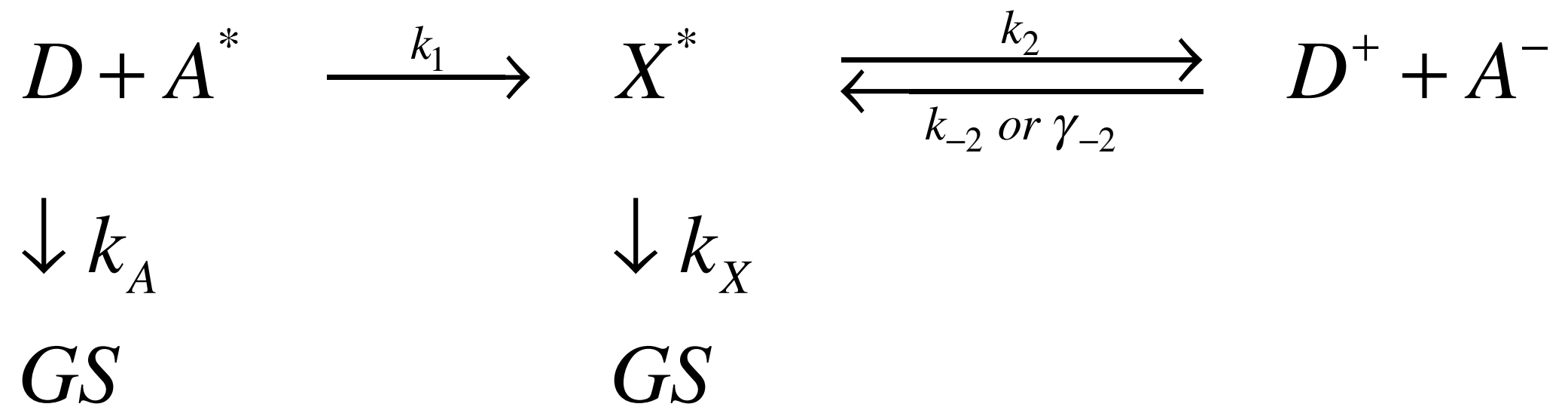
1. Energy loss associated with exciton dissociation
2. Charge generation mechanism at interface



Transient Absorption

Photoluminescence

Microwave
Conductivity

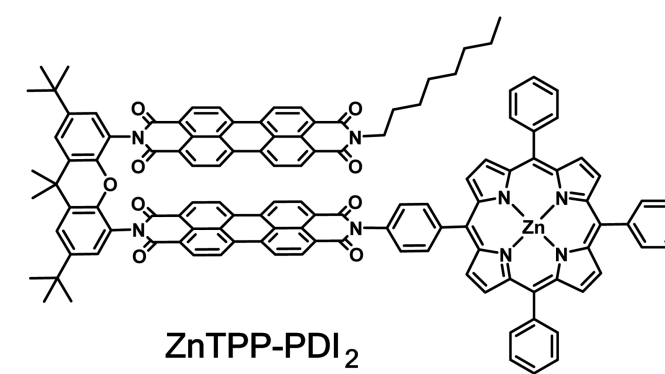
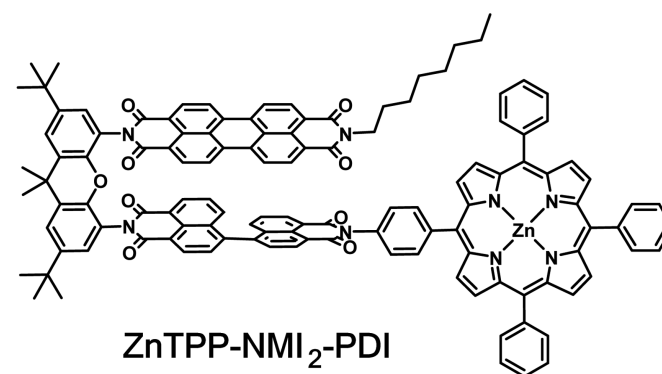
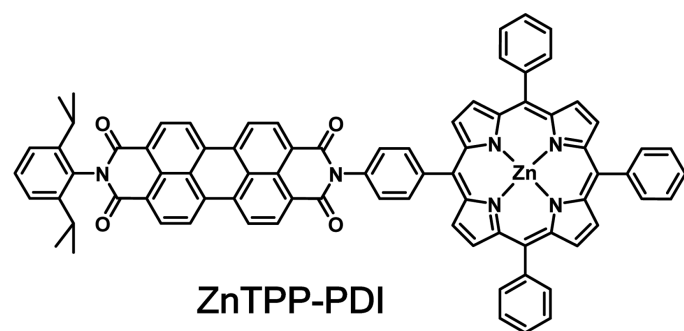


Transient Absorption

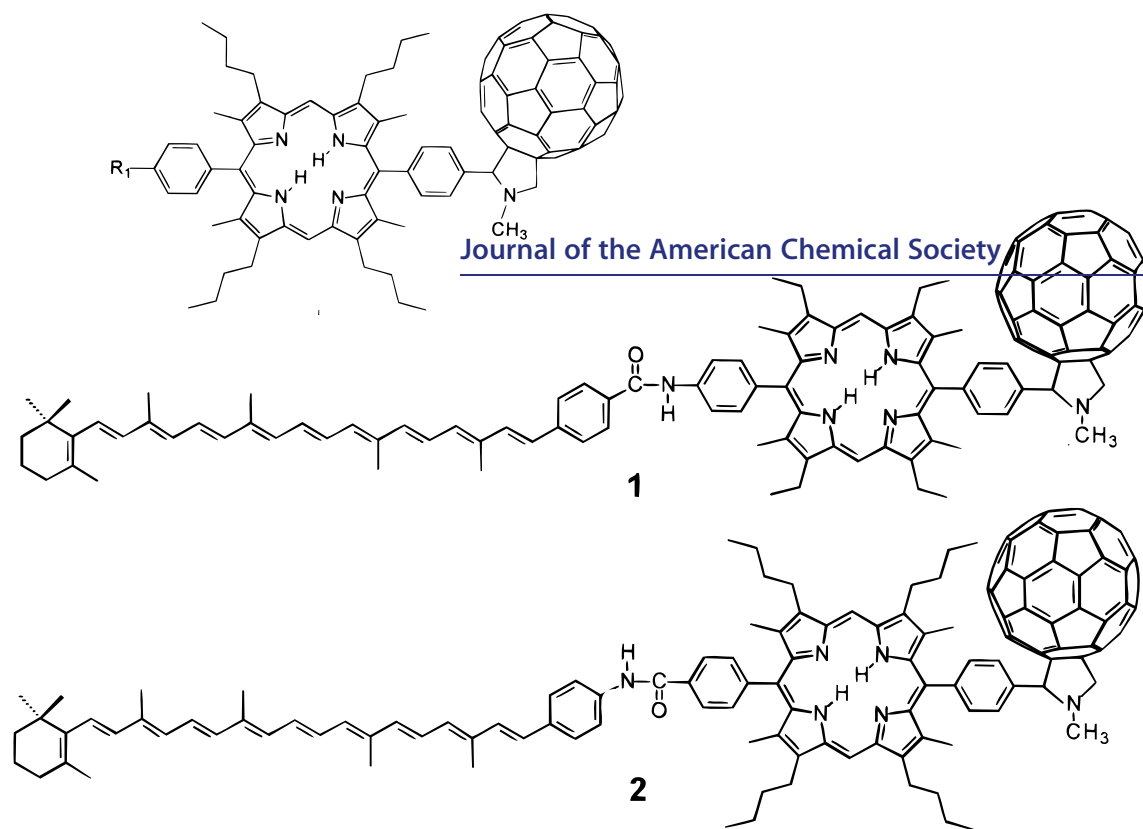
Photoluminescence

Microwave
Conductivity

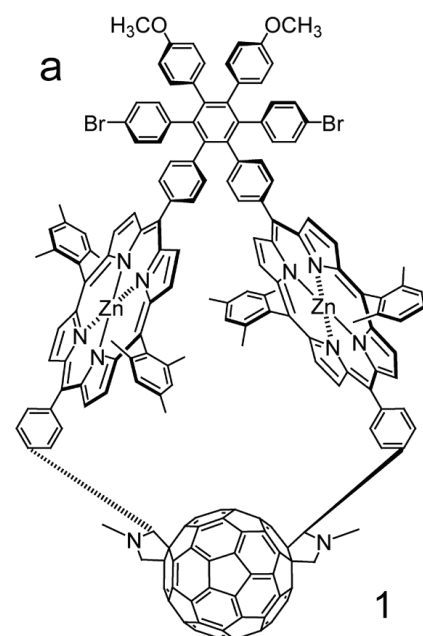
P. E. Hartnett, C. M. Mauck, M. A. Harris, R. M. Young, Y.-L. Wu, T. J. Marks and M. R. Wasielewski, *J Am Chem Soc*, 2017, *jacs.6b10140*.



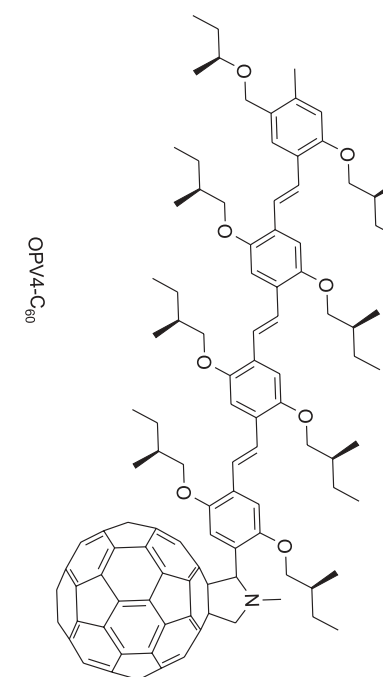
D. Kuciauskas, P. A. Liddell, S. Lin, S. G. Stone, A. L. Moore, T. A. Moore and D. Gust,
J Phys Chem B, 2000, 104, 4307–4321.



V. Garg, G. Kodis, M. Chachisvilis, M. Hambourger, A. L. Moore, T. A. Moore and D. Gust,
J Am Chem Soc, 2011, 133, 2944–2954.

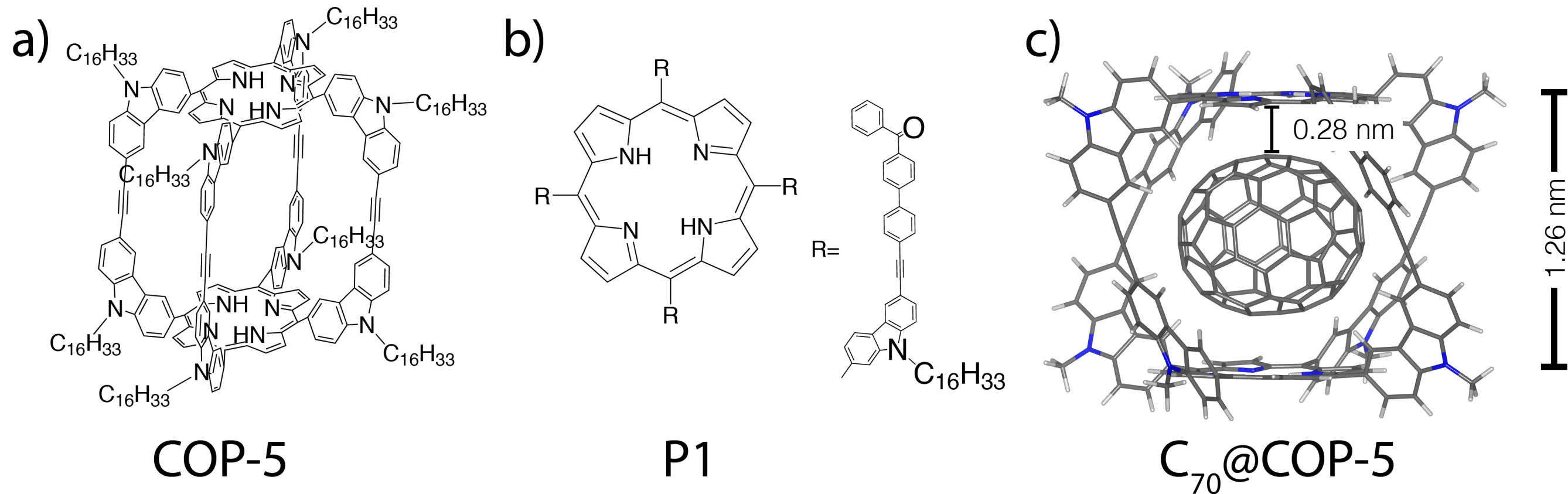


P. A. van Hal, S. C. J. Meskers and R. A. J. Janssen,
Appl Phys A-Mater, 2004, 79, 41–46.

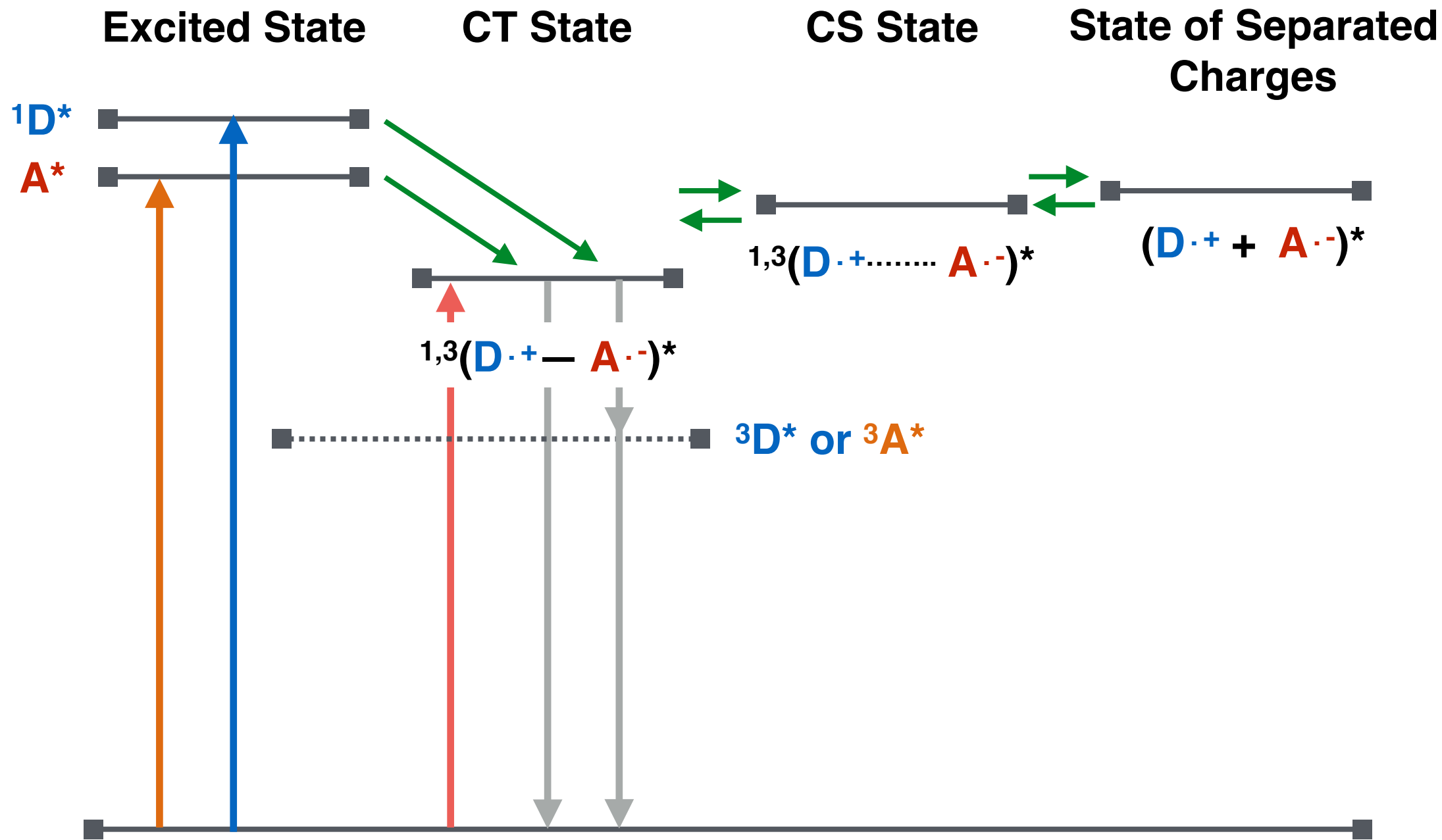


All in low dielectric constant solvents (<7.6)

Zhang, C., Wang, Q., Long, H., & Zhang, W. (2011).
A Highly C₇₀ Selective Shape-Persistent Rectangular Prism Constructed through One-Step Alkyne Metathesis.
Journal of the American Chemical Society, 133(51), 20995–21001.



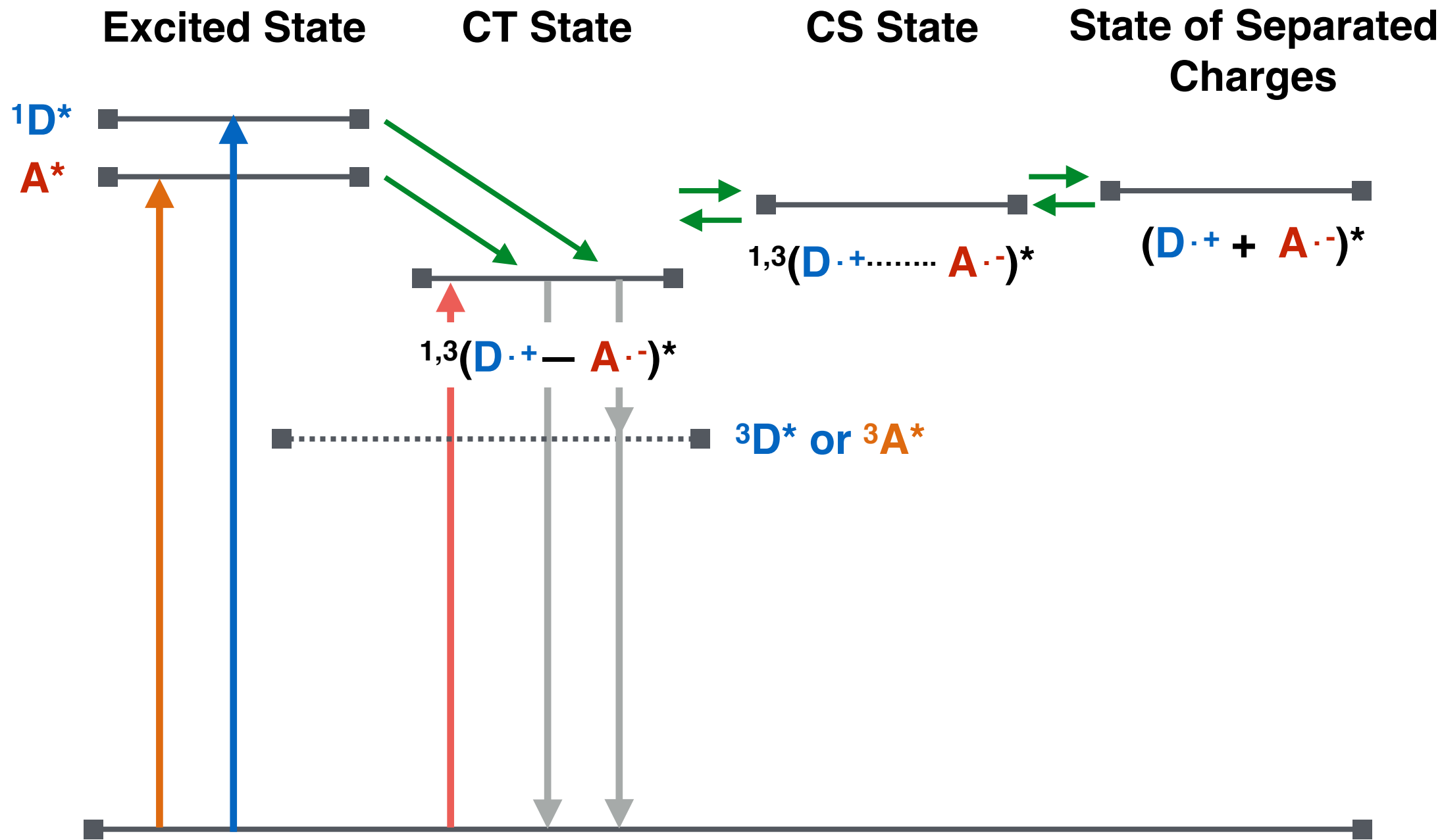
ΔG_{CS} in toluene = -0.27 eV; ΔG_{CS} in Benzonitrile = -0.95 eV



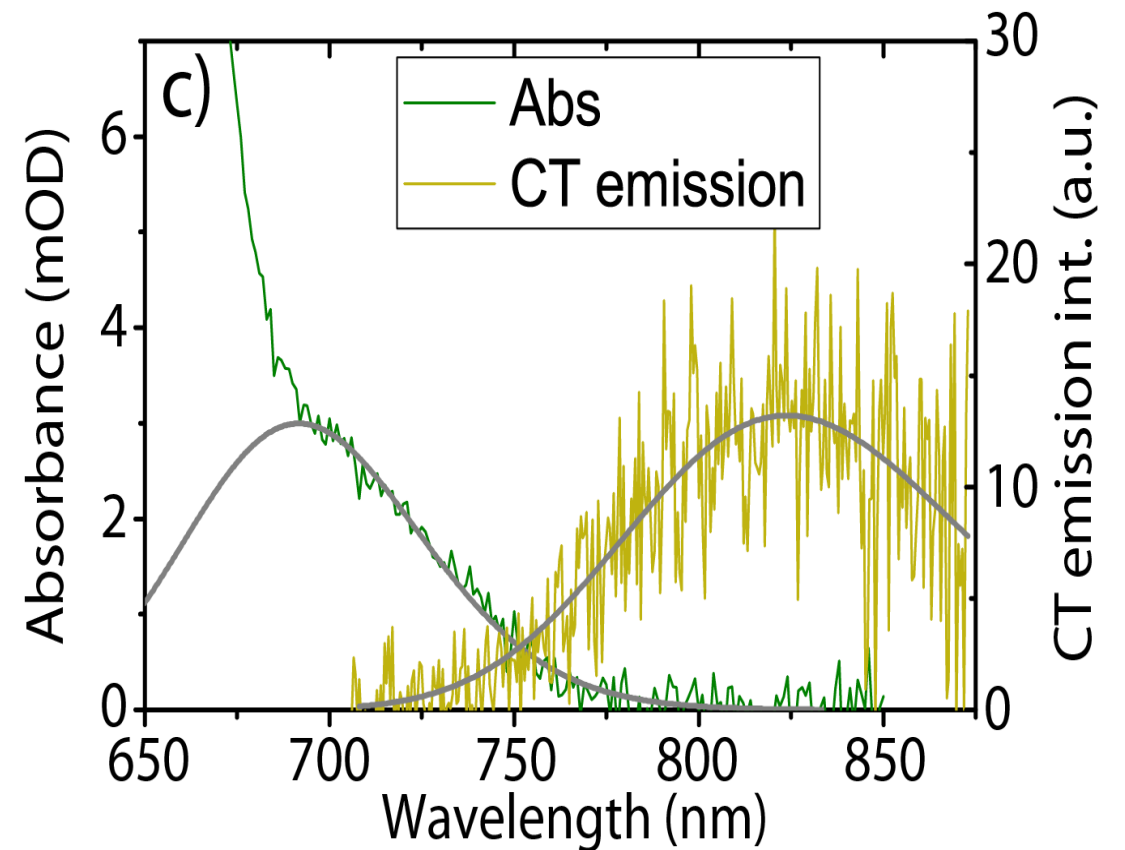
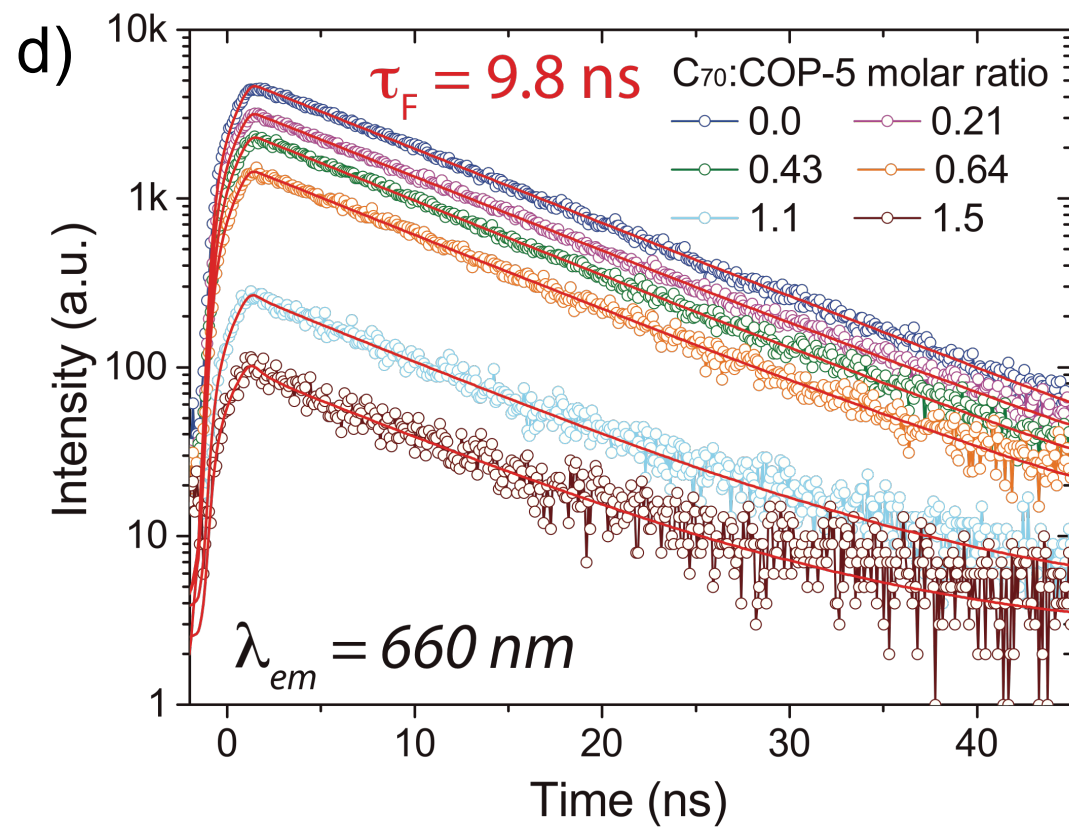
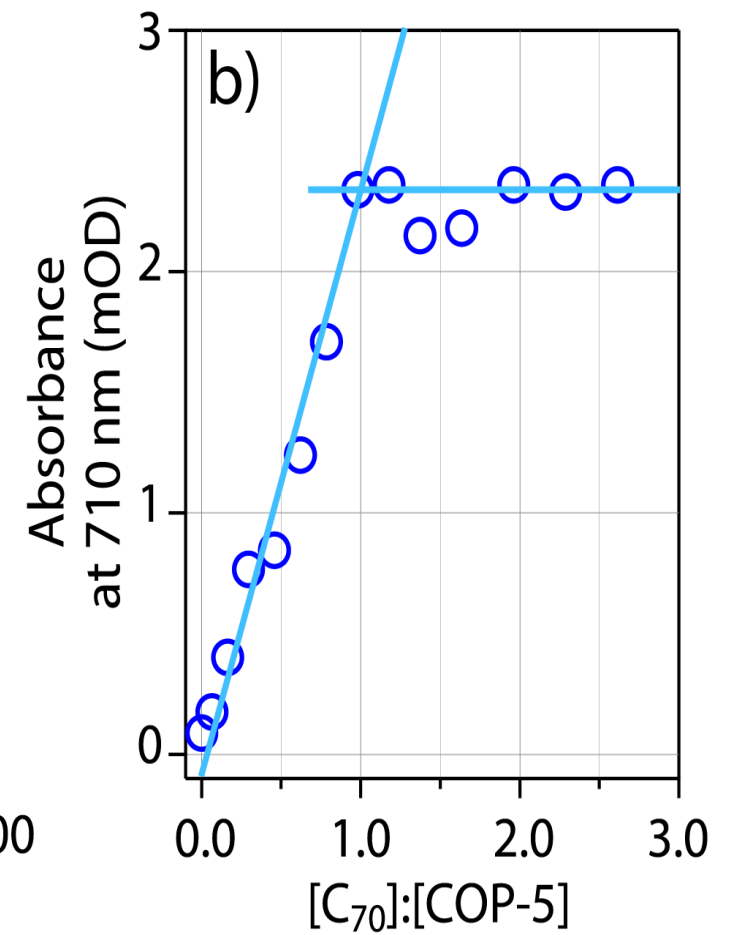
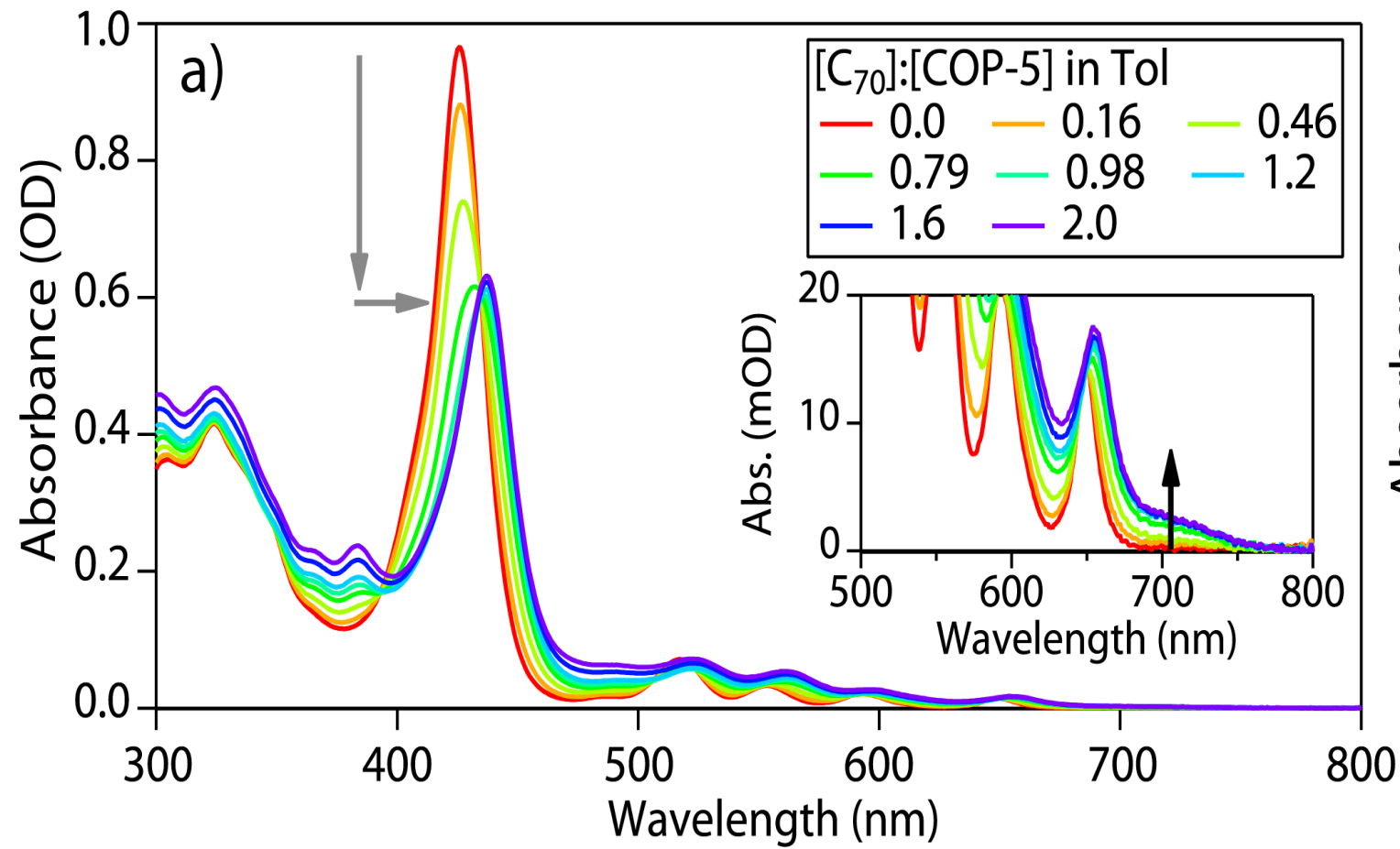
$$\Delta_{ET} G^o = N_A \left\{ e \left[E^o(D^{\cdot+} / D) - E^o(A / A^{\cdot-}) \right] + \frac{z(D^{\cdot+}) z(A^{\cdot-}) e^2}{4\pi\epsilon_0 \epsilon_r a} \right\} - \Delta E_{0,0}$$

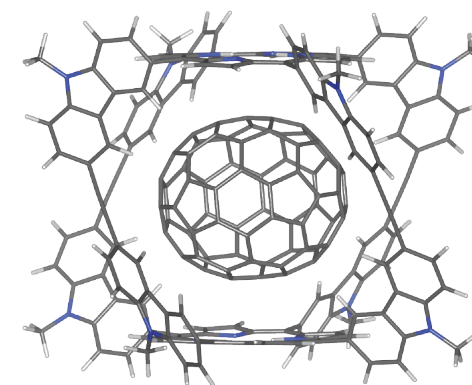
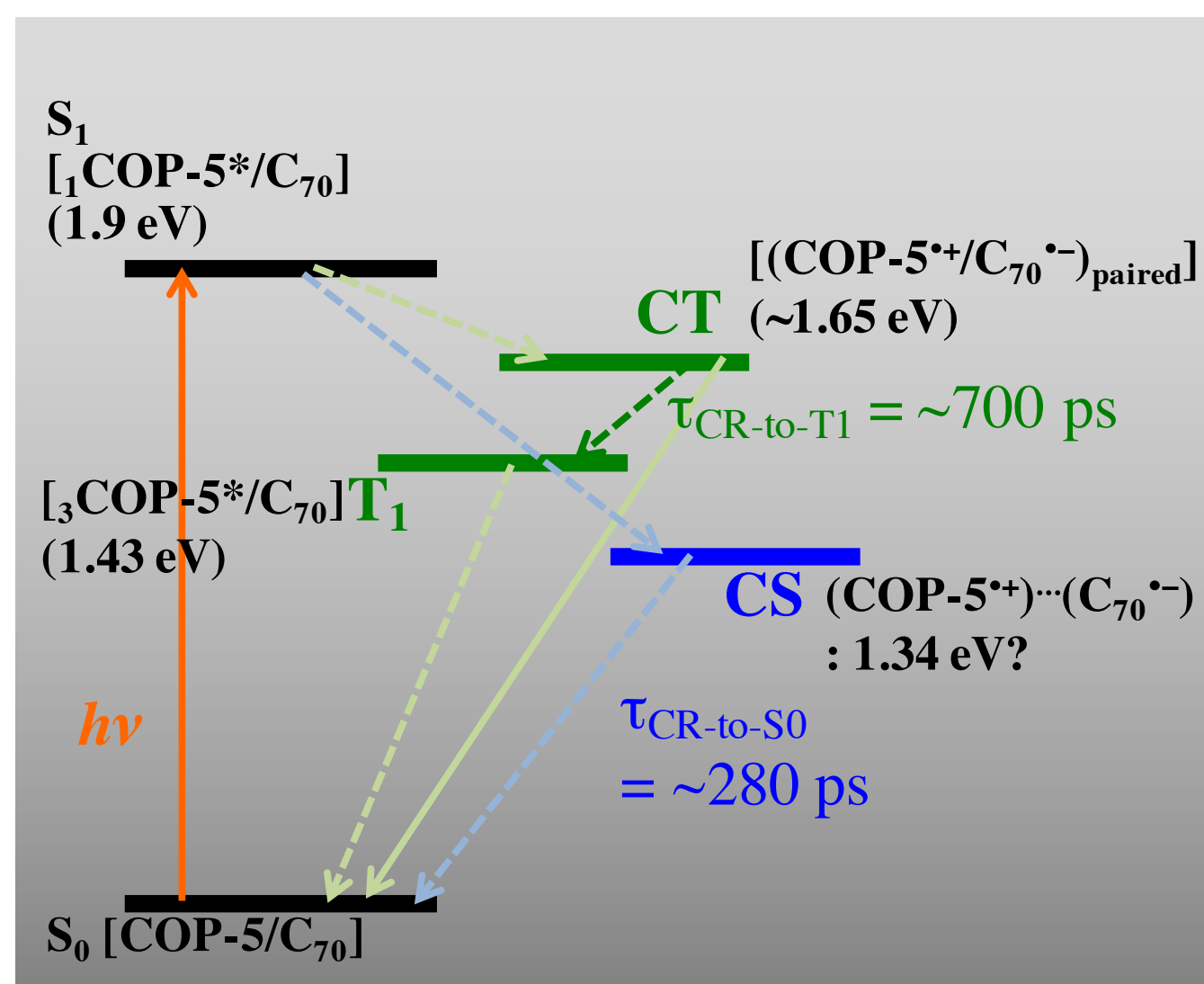
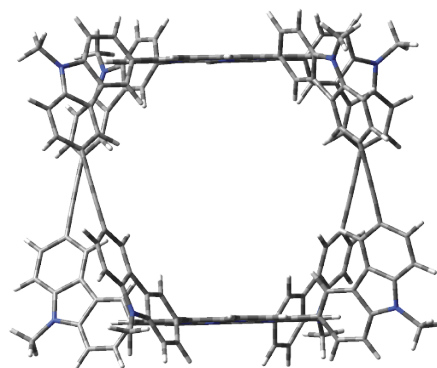
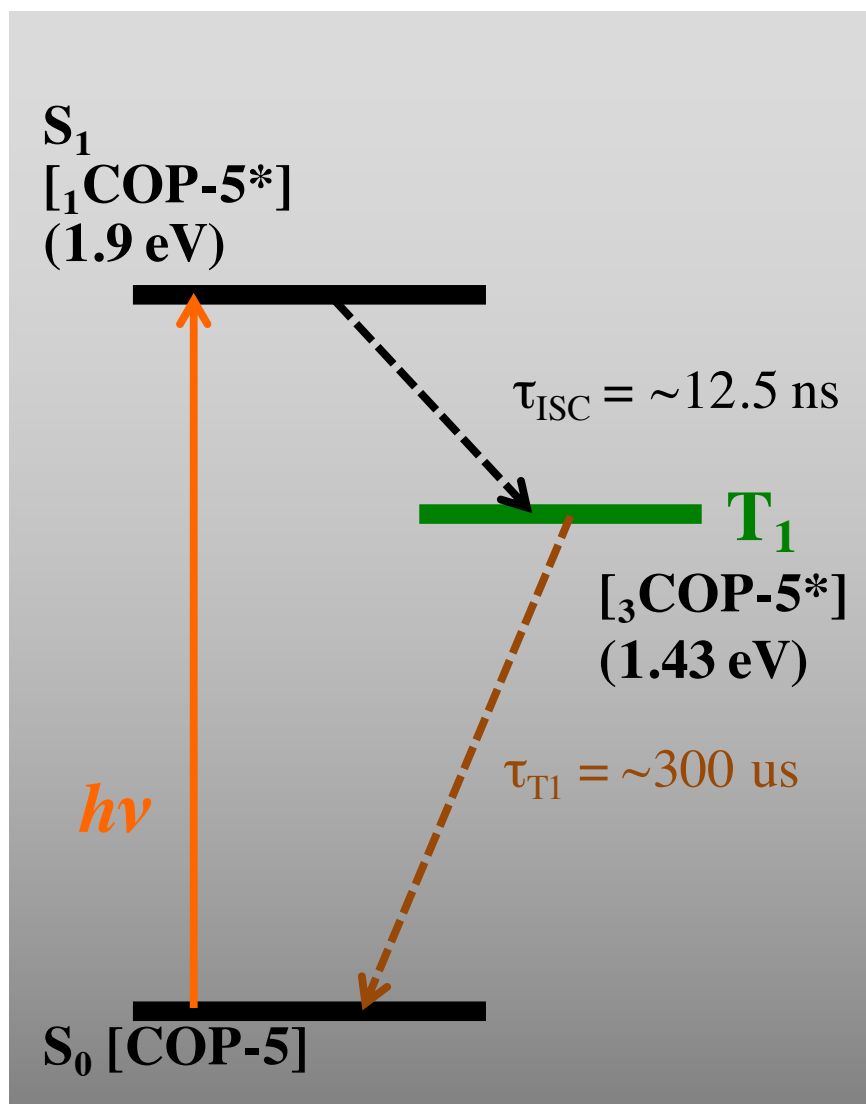
$$\Delta_{ET} G^o = IP_D - EA_A - \frac{e^2}{4\pi\epsilon_0 \epsilon_r a} - E_{Exciton}$$

$$\Delta G_{CS} = (IP_D - E_{Exciton}) - EA_A = LUMO_D^{opt} - LUMO_A^{elec}$$



$$\Delta_{ET} G^o = N_A \left\{ e \left[E^o(D^{\cdot+} / D) - E^o(A / A^{\cdot-}) \right] - \Delta E_{0,0} + \frac{z(D^{\cdot+})z(A^{\cdot-})e^2}{4\pi\epsilon_0\epsilon_r r_{DA}} - \frac{z(D^{\cdot+})z(A^{\cdot-})e^2}{4\pi\epsilon_0} \left(\frac{1}{2r_D} + \frac{1}{2r_A} \right) \left(\frac{1}{\epsilon_{EC}} - \frac{1}{\epsilon_S} \right) \right\}$$



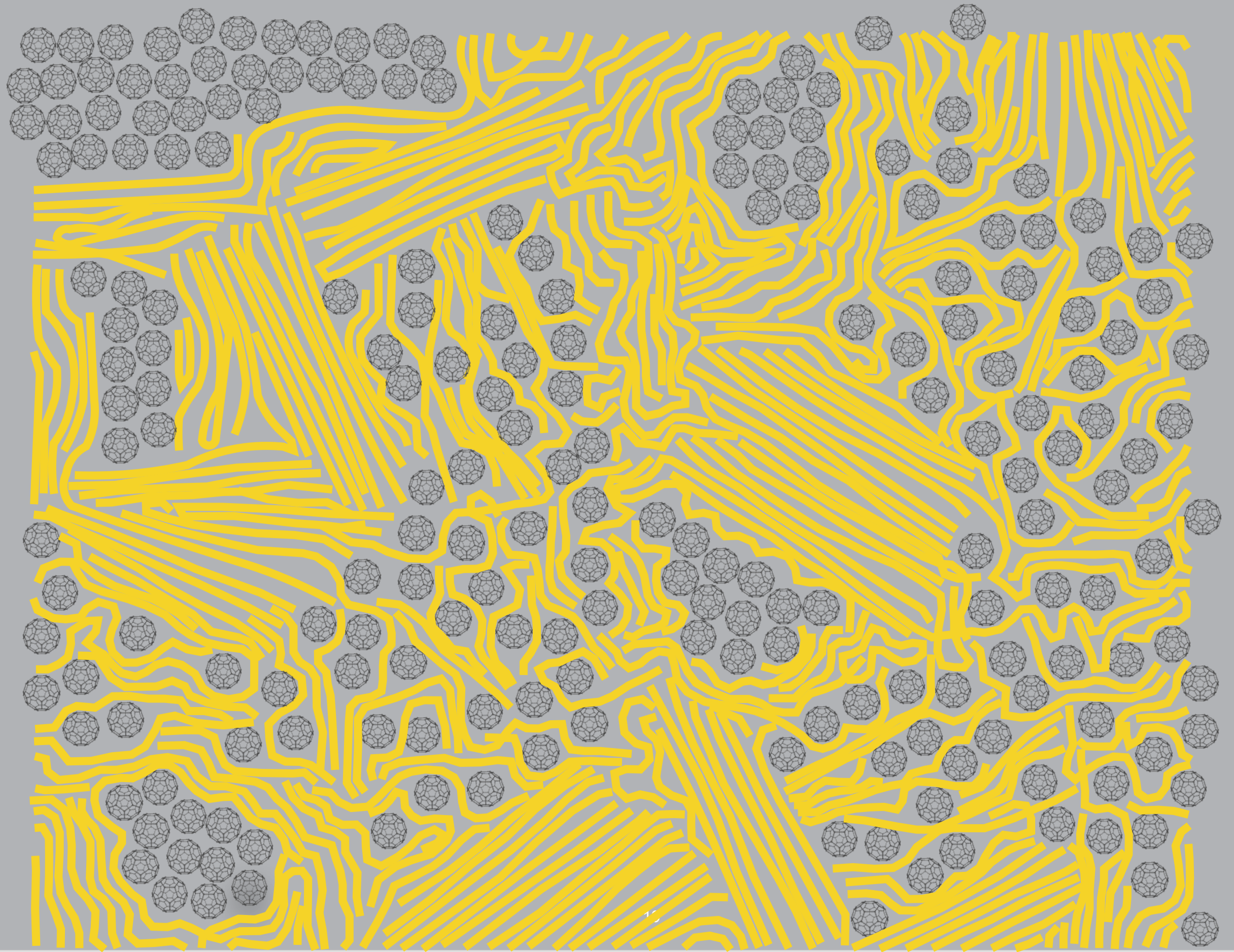


Long-lived charge-transfer state of a C₇₀-encapsulated bisporphyrin covalent organic polyhedron in a low dielectric medium.

Michael Ortiz, Sung Cho, Jens Niklas, Seonah Kim, Oleg G. Poluektov, Wei Zhang, Garry Rumbles, Jaehong Park

J. Am. Chem. Soc. 2017, 139, 4286–4289

A complex conjugated polymer:fullerene blend



- *Research cell efficiencies*
 - Notable exceptions
 - Device area
 - Certification
 - Nanostructured Materials for Type III Photovoltaics; Skabara, P., Malik, M. A., Eds.; The Royal Society of Chemistry, 2018; pp P001–P514.
- *Driving force for electron transfer and the relationship to V_{oc}*
 - Weller equation and Gibbs energy, not LUMO offset
 - Reorganiz(s)ation energy v ΔG
- *Charge-Transfer states, Charge-Separated states, and the state of separated charges*
 - CT states absorb and emit
 - CS states absorb very weakly, are generally associated with molecular triads and photosynthesis reaction center
 - State of separated charges are free of coulomb attraction, are extracted by devices and can b be readily detected using microwave conductivity
- *IP , E_A , v E_{ox} , E_{red}*
 - *Caution with connecting or combining these data*



Search NREL.gov SEARCH

Careers

- FIND A JOB ▾
- YOUR CAREER AT NREL ▾
- POSTDOCTORAL OPPORTUNITIES ▾
- INTERNSHIPS ▾

» Careers » Director's Postdoctoral Fellowship

Postdoctoral Opportunities

Director's Fellowship

Director's Postdoctoral Fellowship

Have you completed your Ph.D. within the last two years? Can you demonstrate a promising career of research and leadership?

The NREL Director's Fellowship attracts the next generation of exceptionally qualified scientists and engineers with outstanding talent and credentials in renewable energy research and related disciplines. One of the fellowship positions is named the Nozik Fellowship, in recognition of Emeritus Senior Research Fellow Dr. Arthur J. Nozik and his outstanding scientific contributions to renewable energy.

Interested in fellowship positions?

Fellowships are available in three disciplines. Please apply to your area of interest.

- SCIENTIST
- ENGINEER
- ANALYST

The Director's Fellowship application process is held four times a year as follows:

Application Window Opens	Application Window Closes*
March 1	July 1

Additional application windows to be determined.
*Applications submitted after the closing date will not be reviewed.

Candidates are selected based on eligibility, program expectations, and research proposals. Overriding consideration, when evaluating the application, will be the quality of the candidate. Successful candidates will serve a two-year term, with a possible third-year renewal paid with program funding (maximum three-year appointments). The Director's Fellowship includes a premium salary rate, additional funding for conferences/presentations, competitive benefits package, and relocation assistance (for moves greater than 50 miles from NREL).

